**Proceedings of the ASME 2012 International Design Engineering Technical Conferences &
Computers and Information in Engineering Conference
IDETC/CIE 2012
August 12-15, 2012, Chicago, IL, USA**

DETC2012-71289

Mobility Determination Of Mechanisms Based On Rigidity Theory

Slavutin Michael
School of Mechanical Engineering
Faculty of Engineering
Tel Aviv University
Tel Aviv, Israel

Offer Shai
School of Mechanical Engineering
Faculty of Engineering
Tel Aviv University
Tel Aviv, Israel

Andreas Müller
Institute of Mechatronics
Technical University
Chemnitz Germany

ABSTRACT

Rigidity theory deals mostly with the topological computation in mechanical systems, i.e. it aims at making generic statements. Mechanism theory is mainly concerned with the geometrical analysis but again also with generic statements. Even more so for mobility analysis where one is interested in both the generic mobility and that of a particular mechanism. In rigidity theory the mathematical foundation is the topology representation using bar-joint and body-bar graphs, and the corresponding rigidity matrix. In this paper novel geometric rules for constructing the body-bar rigidity matrix are derived for general planar mechanisms comprising revolute and prismatic joints. This allows, for the first time, the treatment of general planar mechanisms with the body-bar approach. The rigidity matrix is also derived for spatial mechanisms with spherical joints. The bar-joint rigidity matrix is shown to be a special case of body-bar representation. It is shown that the rigidity matrices allow for mobility calculation as shown in the paper. This paper is aimed at supplying a unified view and as a result to enable the mechanisms community to employ the theorems and methods used in rigidity theory. An algorithm for mobility determination -the pebble game- is discussed. This algorithm always finds the correct generic mobility if the mechanism can be represented by a body-bar graph

Keywords Rigidity theory, generic mobility, body-bar, bar-joint, pebble game

INTRODUCTION

One of the unsolved problems in mechanism theory is the mobility determination for mechanisms with arbitrary geometry and topology. This has always been a topic of continuous research. Although nowadays the problem is well-understood there is still to this day holistic and universal mobility criterion. The problem impeding such a universal criterion can be summarized in one word: redundancy. This may be due to a special geometry or inherent to the topology. Figure 1a) shows the well-known geometrically redundant (overconstrained, paradox) Bennett mechanism, which has 1 DOF. Any mechanism with the same topology but general geometry is immobile. Also the planar mechanism in figure 1b) has 1 DOF but this is topologically redundant in the sense that its mobility would not change if, e.g. bar AC would be removed. This redundancy is preserved for any mechanism with this topology regardless of the particular geometry.

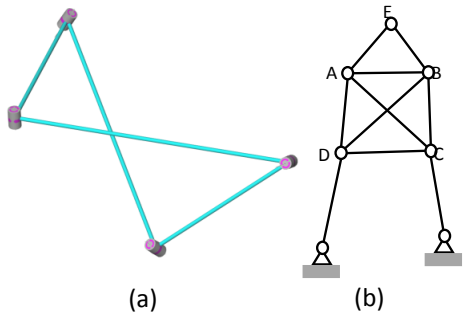

Figure 1 (a) The 1 DOF overconstrained (geometrically redundant) Bennett mechanism; (b) Example of a topologically redundant 1 DOF mechanism

Historically, mechanism theory has mainly been concerned with geometrically overconstrained mechanisms [2,3,7,8, 11,15,16,28,29,], whereas topological redundancy is traditionally a topic of rigidity theory [26,32]. This pending division has led to the development of different approaches but it turns out that methods from rigidity theory can also be successfully employed for the mobility analysis of mechanisms.

The approaches to mobility determination in mechanism theory can be roughly divided into three classes: 1) those that aim to solve the kinematic relations, 2) those taking into account motion characteristics, and 3) topological methods. The mobility of a specific mechanism is a geometric property that is More precisely the local mobility of a mechanism in a given configuration is the local dimension of the c-space at this particular configuration [17,18]. The explicit resolution of the kinematic relations of a specific mechanism is the most natural approach [28,29],[33] ,[34]. The difficulty arises from the non-linear nature of the problem, that impedes the explicit solution for general mechanisms, and one needs to resort to the first-order analysis using Jacobians and screw systems. The latter does in principle only reveal the first-order instantaneous mobility, however, but it is shown in [5, 6] that also the finite mobility can be determined by incorporating the Jacobian rank condition in the solution method. Even if the solution set, i.e. the c-space, cannot be determined explicitly, the local mobility can be deduced from a higher-order approximation. Such higher-order approximations, up to any order, are given in terms of Lie brackets of the joint screw coordinates [19]. It is known that a mechanism may have different local mobilities, i.e. it may attain a different finite mobility after a finite motion without disassembling it. Such mechanisms are termed kinematotropic [33]. This is revealed by a higher order approximation of the c-space. In this regard, the definition of higher-order rigidity and shakiness has been reported [24]. Another recent class of approaches that falls into this category makes use of methods from algebraic geometry. The basic idea is to determine the dimension (and possibly a local approximation of the c-space) of the configuration space by means of advanced algorithms from numerical algebraic geometry [9,20,1]. The second class makes use of the concept of motion groups [7, 8]. Instead of aiming atthe solution of the constraints, the dimension of the c-space is estimated upon the dimension of the motion spaces associated the mechanism's screw system, more precisely that of independent kinematic loops [21]. The latter are exactly the parameter g in the formula (1) below. Methods of the third class are concerned with the kinematic topology, i.e. the arrangement of bodies and joints, rather than with the particular geometry or motion characteristics. In fact no aspects of feasible motions are taken into account, and the aim of these methods is to determine the *generic mobility*, i.e. the most likely mobility of a mechanism with a given topology when freely choosing its link geometry. The best-known representative of this class is the Chebyshev-Kutzbach-Grübler (CKG) formula. Methods encoded in its configuration space (c-space).like the CKG formula are attractive since they promise to quickly yield the generic mobility without the need to specify geometric parameters, and are therefore widely used. At the same time it is well-know that the CKG formula (and all its variants) fails in many situations that have been deemed exceptional. However, many such 'exceptional' systems are used in practice, which calls for an alternative to the CKG formula. Such an alternative is the use of a combinatorial method, called the Pebble game algorithm that was developed in the context of rigidity theory [23]. This method requires an appropriate graph representation of the kinematics, namely body-bar and bar-joint graphs, as will be explained in this paper. Beside their relevance for the pebble game algorithm these graph representations give rise to the so-called rigidity matrix -the central object in rigidity theory. Currently the rigidity theory approach is limited in that it only allows for spherical joints. In this paper the necessary constraints for prismatic joints are derived that enable extension of the body-bar approach to general planar systems. To the authors' knowledge the mechanism analysis using body-bar graphs has not been reported so far.

The paper is organized as follows. In section 2 the topology representation used in mechanism theory and the CKG formula is recalled. Section 3 gives a brief review of basic facts from rigidity theory. The two relevant types of representations-body-bar and bar-joint graphs- are discussed in section 4 and 5, respectively. For each representation the corresponding rigidity matrix is introduced. As a main contribution of this paper, the rules for constructing the rigidity matrix are derived for planar mechanisms comprising revolute, in-line, and prismatic joints, as well as distance constraints, and for spatial mechanism comprising spherical joints are derived. It is explained how the rigidity matrix can be used for mobility determination. In section 6 the pebble game algorithm is described in some detail. Its potential use and limitations are discussed. The paper concludes with a summarizing discussion in section 7.

2 Topology Representation and the CKG-Formula

The essential object for the use of topological methods is the representation of the mechanism topology. In mechanism theory and multibody dynamics the kinematic topology of a

mechanism is commonly represented by a non-oriented graph Γ(V,E),where a vertex $v \in V$ represents a rigid body and an edge $e \in E$ stands for a joint, connecting exactly two bodies, regardless of the DOF of the joint (figure 1). This representation of the mechanism kinematics accounts for the arrangement of joints and bodies. It does, however, not explicitly take into account the number of constraints imposed by the individual joints. These can indirectly be indicated by assigning a weight to each edge. This gives rise to well-known CKG formula

$$\delta = \sum_{i=1}^{J} f_i - g(J - B + 1) \qquad (1)$$

Where J is the number of joints, B is the number of bodies, and f_i is the DOF of joint i (the weight of edge i). The parameter g is adjusted to the 'type' of the mechanism, or conversely different types of kinematic loops can be realized. This 'type' of mechanism pertains essentially to the motion group associated with a mechanism or to a kinematic loop, i.e. sub groups of the rigid body motion group $SE(3)$. Hence possible values of g are1,2,3,4, and 6. Common choices for this parameter are g=6 for spatial mechanisms, and g=3 for planar and spherical mechanisms.This formula has appeared in various forms, and was amended in order to capture redundancies. An exhaustive overview and historical perspectives were reported in [4].

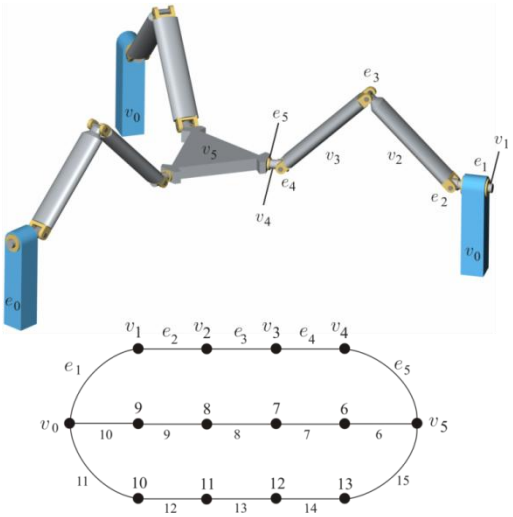

Figure 2 The topological graph of a parallel manipulator. Vertices v_i represent bodies and edges e_i represent joints

If higher DOF joints are replaced by a sequence of 1-DOF joints, then the CKG formula can be rewritten as

$$\delta = n - g\gamma \qquad (2)$$

where n is the number of 1-DOF joints, and $\gamma = J - B + 1$is the number of fundamental loops of Γ (Euler's number, cyclomatic number).

The mobility determination of mechanisms that are not geometrically over-constrained boils down to identifying topologically redundant subsystems. It turns out that the above topology representation is not adequate for this purpose. On the other hand there are now combinatorial methods from rigidity theory for identifying topological redundancy and redundant rigid substructures (identification of topological self-stress). The mathematical foundation is Laman's theorem [12] and the algorithmic tool is the pebble game algorithm [10]. They make use of two further concepts for representing the mechanism kinematics, namely the *body-bar* and *bar-joint* graphs.

The CKG formula only uses topological information but no information about the specific geometry. Albeit being simple, the CKG-formula fails for special geometries and topologies since it neither respects the geometry nor the topological redundancies. Mechanisms exhibiting either characteristic are collectively called *over-constrained* (redundantly constrained).It was shown in [17]that the CKG-formula yields generically the correct mobility provided that the mechanism is not topologically redundant. The attribute generic refers to mechanisms with general geometry, i.e. not subject to additional conditions. In other words a mechanism is generic if it is not geometrically over-constrained. Now, the question arises whether there is a method to deduce the correct *generic mobility* from the topological information even for topologically redundant systems. The preliminary answer is: Yes, if the mechanism can be represented by a body-bar graph.

The reason why the topological graph (which is the foundation for the CKG formula) is not adequate for combinatorial mobility determination is that it lags the information about the number of constraints imposed by the individual joints. Now, alternatively the body-bar graph, for instance, does account for the joint constraints. The difference is that in the body-bar graph each edge (bar) stands for exactly one constraint as discussed below. The importance of this representation is that it does allow to treat topologically redundant systems, unlike the CKG formula.

The core aim of this paper is to show the potential of using representations and methods from rigidity theory for mobility computations. In the following sections these approaches are discussed and are shown to be related to each other, and their limitations are outlined. Emphasize is put on the involved rigidity matrices and their kinematic background. In particular the constraint formulation for spherical joints is recalled, and a novel formulation for prismatic joints is presented.

3. Review of Rigidity Theory Approaches to Mechanism Analysis

Rigidity theory is a combinatorial theory that encompasses topological theorems and methods that are used in order to prove whether the graphs, or the corresponding physical systems represented by the graphs, are rigid or mobile. Note, most of the works in rigidity theory deal with topological considerations, i.e., when a graph is concluded to be rigid it signifies that it is generically rigid without giving consideration to any specific geometry.

The main work initiated in 1970, by the work of Laman [Lam] where he proved the necessary and sufficient condition for a graph in 2D to be rigid, commonly known as the ***Laman theorem***:

Theorem 1 Let G be a graph with v(G) vertices and e(G) edges, such that e(G)=2*v(G)-3. G is rigid in 2Diff for any sub-graph of G'

$$e(G') \leq 2*v(G') - 3. \quad (3)$$

As an example, the graph in Figure 2a is not rigid since the subgraph with the vertices {B,C,D,E} has six edges and four vertices, thus: 6>2*4-3, contradicting equation 2.

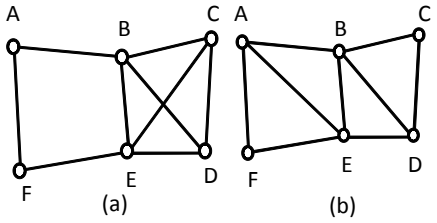

Figure 2 (a) This graph is not rigid thus it does not satisfy Laman's theorem. b) A rigid graph.

The main downfall of this theorem is that it requires an exponential number of checks for all the possible sub-graphs, thus it is impractical to computerize it. Ever since the publication of Laman, many well-known mathematicians have toiled to find a polynomial run-time algorithm for checking the rigidity of graphs, and many equivalent theorems for Laman's theorem were developed which theoretically require only a polynomial number of checks, but were very complicated. Among them, is the work reported in 1982 in which for multiplying any edge there is a need to find two disjoint spanning trees [14].

The work in rigidity theory strongly relates to mechanical engineering since they talk about the topological DOF of the graphs. Note, the graphs correspond to physical systems that are floating, i.e. ungrounded/not pinned. In the light of rigidity theory, kinematic chains with revolute joints can be termed floating linkages, and mechanisms can be termed pinned linkages. Thus, checking whether a mechanism has one topological DOF can be referred to in rigidity theory as checking whether the corresponding pinned graph after grounding the drivers is rigid.

In 1997, a very efficient algorithm for checking a variant of Laman's theorem was developed and implemented in computer software, called ***the pebble game*** **[10]**, explained in detail later in section 5. Succinctly, the pebble game verifies whether a graph satisfies Laman's condition in a polynomial time. Moreover, pebble game can determine the topological DOF of any graph, determine the DOF of every vertex, indicate the redundant regions and decompose the graph into Assur Graphs [22].

Albeit the success in 2D, the situation is 3D is much more complicated. Laman's theorem in 3D is as follows.:

Theorem 2 Let G be a graph with v(G) vertices and e(G) edges, such that e(G)=3*v(G)-6. G is rigid in 3D if for any sub-graph of G'

$$e(G') \leq 3*v(G') - 6 \quad (4)$$

This theorem was found to be insufficient for 3D graphs. For example, the double banana [31], which although satisfies the 3D Laman's theorem is not rigid

Alternatively to the combinatorial pebble game algorithm the body-bar and bar-joint representations also allow for mobility determination using the so-called rigidity matrix. This is explained in section 4 and 5, respectively.

4 The Body-Bar Approach to Mechanism Analysis

4.1 The Body-Bar Graph

The body-bar approach uses a graph representation where vertices represent bodies and an edge represents exactly one scalar constraint restraining the relative motion of the two bodies it is connected to. E.g. a revolute joint in 2D is represented by two constraints (edges), a spherical joint in 3D by three, hinges by five and so forth. Consider the planar mechanism in figure 3a. Its body-bar graph is shown in figure 3b). It is common practice to visualize the nodes, i.e. the bodies, by polygons. Body 4 is connected to the ground by a revolute joint, denoted J4. The latter imposes two translation constraints (in the plane) to body 4. This is reflected in the body-bar graph by two edges between the ground and body 4 denotedJ4x and J4y. The higher pair C, on the other hand, only imposes one constraint represented by the edge C in figure 3b. Further imposed motions can be easily included by an additional edge such as the motion imposed by the driver link in figure 3.

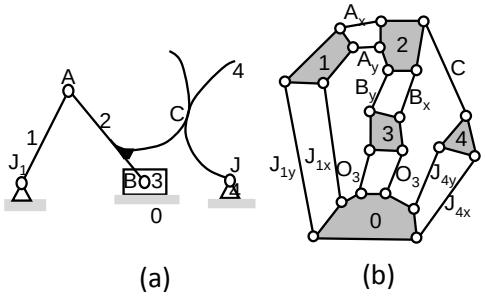

Figure 3 The body-bar graph (b) corresponding to a mechanism (a)

The body-bar graph of spatial mechanisms is similar, and comprises for example five and three edges for each hinge and spherical pair, respectively.

In summary, the body-bar graph is an abstract representation of the constraints imposed to the bodies of a mechanism. This formal representation of the constraint equations, and hence of the kinematic topology, is suited for algorithmic treatment of kinematics. Even more, since each edge corresponds to exactly one scalar constraint, it can be used to determine the generic, i.e. topological, mobility of mechanisms.

There is extensive ongoing research on this type of graphs and novel applications [31]. The advantage of using body-bar graphs is that it is mathematically proved [25] that the generic DOF can be calculated for any spatial system, where the CKG-formula fails. In other words, when a mechanism is presented by body-bar graph there exist combinatorial algorithms, such as the pebble game, that find the correct mobility. Note, for bar and joint graphs there exist algorithms that find the correct generic mobility only for 2D.

4.2 The Corresponding Constraints

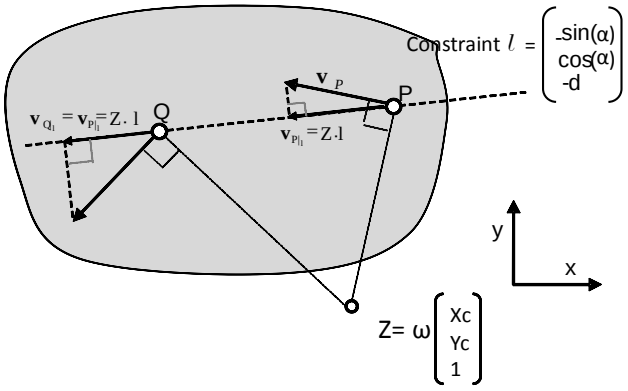

Figure 3 The main property of body-bar mechanisms.

In the following a few results from planar projective geometry are needed that have been summarized in the appendix. Throughout the paper capital letters denote homogeneous coordinates. Denote with C the homogenous coordinates of the instantaneous center of motion, and introduce $Z = \omega C$.

The main property underlying the body-bar analysis is the following:

Property 1: The length of the projection of the velocity of any point P, onto a line(not at infinity) with coordinates l, denoted by $v_{P|_l}$, is equal to the scalar product of Z, with the line coordinate vector: $v_{P|_l} = Z \cdot l$.

To prove the above statement consider some line with coordinates l that passes through a point P of the body.If $\mathbf{e}_l$ is the unit vector along the line, then the magnitude of the projection of the velocity of point P on the line is:

$$v_{P|_l} = \mathbf{v}_P \cdot \mathbf{e}_l = v_{P_x}\cos\alpha + v_{P_y}\sin\alpha = \omega(y_C - y_P)\cos\alpha + \omega(x_P - x_C)\sin\alpha =$$
$$= \omega(-x_C\sin\alpha + y_C\cos\alpha + x_P\sin\alpha - y_P\cos\alpha) =$$
$$= \omega\begin{pmatrix} x_C & y_C & 1 \end{pmatrix}\begin{Bmatrix} -\sin\alpha \\ \cos\alpha \\ x_P\sin\alpha - y_P\cos\alpha \end{Bmatrix} = \omega\begin{pmatrix} x_C & y_C & 1 \end{pmatrix}\begin{Bmatrix} -\sin\alpha \\ \cos\alpha \\ -d \end{Bmatrix} = Z \cdot l \qquad (5)$$

It may be noted that this projection does not depend explicitly on the point P, but only on the line *l*and the center of motion of the body, represented by Z. Thus, for any point of the rigid body that lies on the line *l* the projection of the velocity on this line is the same as shown in figure 3 where the two points P and Q have the same projection. This is a well-known property of the rigid body [32].

Property 1 can now be applied to the analysis of body-bar graphs. As mentioned above, each body is constrained by lower or higher pairs represented by several edges in the body-bar graph, each corresponding to one constraint. The basic constraints are the following:

a. Driver Constraints: The driver applies a given linear velocity at the joint where the driver is connected to the body. Let A be the joint, $\mathbf{v}_A$ its linear velocity and l_{A_x} the line that passes through point A and parallel to the x-coordinate axis. Thus, according to property 1 the projection of the velocity of point A on line l_{A_x}, the constrained, is:

$$\mathrm{v}_{A_x} = \mathrm{Z} \cdot \mathrm{l}_{A_x} = \mathrm{Z} \cdot (\mathrm{A} \vee \mathrm{i}) = \omega(\mathrm{y}_C - \mathrm{y}_A) \qquad (6)$$

The same applies to the y-component:

$$v_{A_y} = Z \cdot l_{A_y} = Z \cdot (A \vee j) = \omega(x_A - x_C) \qquad (7)$$

Where ***i*** and ***j*** denote the homogenous coordinates of the x and y axis, respectively.

b. The Constraint of a Revolute Joint connecting two Bodies: Let B_I and B_{II} be two bodies connected by are volute jointat point A. Since the velocities of the two bodies at point A are equal, their projections on the two lines l_{A_x} and l_{A_y} through A should be the same, which yields the following equations

$$\begin{aligned} (Z_I - Z_{II}) \cdot l_{A_x} &= 0 \\ (Z_I - Z_{II}) \cdot l_{A_y} &= 0 \end{aligned} \qquad (8)$$

c. The Constraints of a Bar (Binary Link) connecting two Bodies: Let B_I and B_{II} be two bodies connected by a bar along the line $l$that is linked to Body B_I and B_{II} via revolute joint at points A and B, respectively. The bar itself is not treaded as rigid body of the system. Since bar is rigid the projections of its two end joint velocities, $\mathbf{V}_A$ and $\mathbf{V}_B$ on the line $l$must be identical, i.e,

$$0 = \mathbf{v}_{A|1} - \mathbf{v}_{B|1} = (Z_I - Z_{II}) \cdot l \qquad (9)$$

Since the line along the bar is defined by the points A and B it can be expressed with the join operation $l_1 = A \vee B$. Hence the constraint is

$$Z_I \cdot (A \vee B) + Z_{II} \cdot (B \vee A) = 0 \tag{10}$$

d. The Constraint for an Inline Joint

An inline joint at point A restricts the relative motion of two bodies B_I and B_{II} so that they can only translate relative to each other along a line l but can freely rotate. It hence imposes one translation constraint. This models a notch for instance. Let $\mathbf{e}_l$ be a unit vector along the line. The joint restrains the relative translation of B_I and B_{II} perpendicular to $\mathbf{e}_l$. Denote with $\mathbf{e}_l^{\perp}$ a unit vector orthogonal to $\mathbf{e}_l$. Formulating the corresponding constraint requires an expression of the velocity of a point on a body along $\mathbf{e}_l^{\perp}$. The magnitude of the component of the velocity of a point A at a body perpendicular to the line l is

$$\mathbf{v}_A \cdot \mathbf{e}_l^{\perp} = -v_{A_x} \sin\alpha + v_{A_y} \cos\alpha = -\omega(y_C - y_A)\sin\alpha + \omega(x_A - x_C)\cos\alpha$$
$$= \omega \begin{pmatrix} x_A & y_A & 1 \end{pmatrix} \begin{pmatrix} \cos\alpha \\ \sin\alpha \\ 0 \end{pmatrix} - \omega \begin{pmatrix} x_C & y_C & 1 \end{pmatrix} \begin{pmatrix} \cos\alpha \\ \sin\alpha \\ 0 \end{pmatrix} = \omega A \cdot l_\infty - Z \cdot l_\infty \tag{11}$$

where l_∞ denotes the point at infinity approached along l.

The joint constraint is that the projection (11) of the velocities $\mathbf{v}_A^I$ and $\mathbf{v}_A^{II}$ of body B_I and B_{II}, respectively, are equal, i.e.,

$$\mathbf{v}_A^I \cdot \mathbf{e}_l^{\perp} - \mathbf{v}_A^{II} \cdot \mathbf{e}_l^{\perp} = (\omega_1 - \omega_2) A \cdot l_\infty - (Z_1 - Z_2) \cdot l_\infty = 0 \tag{12}$$

Note that the dot products of the homogenous coordinate vectors A and Z_1, Z_2 with l_∞ is nothing but the scalar product of the position vectors with $\mathbf{e}_l$. In (12) any point on the joint axis, i.e. on the line l, can be used. In particular the perpendicular of the origin to the line, or the origin itself, can be used as point A. This yields the final form of the constraints

$$(Z_1 - Z_2) \cdot l_\infty = 0 \tag{13}$$

e. The Constraints for a Prismatic (translational) Joint: A prismatic joint restricts the motion of two bodies to pure translation along its axis. It can be derived from the inline-joint by adding the rotation constraint. Then the two constraints imposed by the joint are

$$\begin{aligned} (Z_1 - Z_2) \cdot l_\infty &= 0 \\ \omega_1 - \omega_2 &= 0 \end{aligned} \tag{14}$$

where ω_1 and ω_2 is the respective angular velocity of body B_I and B_{II}.

With these joint primitives it is possible to model a large number of mechanisms since all lower pairs, except the screw joints, can be represented as succession of revolute and prismatic joints.

4.3 The Body-Bar Rigidity Matrix for Mechanisms and Mobility

The overall set of velocity constraints can be summarized in the following system of linear equations in terms of $Z_i, i = 1, \ldots N$

$$\begin{pmatrix} 0 \\ v \end{pmatrix} = R \begin{pmatrix} Z_1 \\ \vdots \\ Z_N \end{pmatrix} \tag{15}$$

where *v* summarizes the driver velocities. The coefficient matrix R is the so-called *body-bar rigidity matrix*.

In the rigidity matrix *R* the rows correspond to the constraints (bars, driver, turning pairs) and the N columns to the bodies. For each body there are three columns corresponding to $Z_i = (\omega_i x_{ci}, \omega_i y_{ci}, \omega_i)$. Apparently the motion of the system is uniquely determined by the driver velocities *v* iff R has full rank. In particular if the left-hand side of (15) is zero, the system is instantaneously rigid, hence the name of *R*.

Notice that the rigidity matrix reveals whether or not the overall system consisting of the mechanism and the driver constraints is instantaneously determined. Consequently if only the geometric constraints are taken into account for constructing the rigidity matrix (i.e. the drivers are considered passive), the rank of the rigidity matrix does indeed determine the mobility as $\delta = 3N - \mathrm{rank} R$. It is instructive to reflect on this fact since it clearly shows the relation to the rigidity theory. If the rigidity matrix is determined symbolically, then its rank depends on the geometric parameters, and one may deduce the generic mobility. If it is evaluated for particular geometric parameters, one gets the instantaneous mobility of that particular mechanism.

Figure 4 shows exemplary entries in the rigidity matrix for the constraints discussed above.

As an example consider the rigidity matrix of the Stephenson type II mechanism in Figure 5 (note that the crank 0 is not regarded as a member of the mechanism).

In this example three bodies are identified: the ground 0 and the triangles I and II. The centers of motion of the triangles are Z_I and Z_{II}, respectively. The equations are derived by applying the matrix construction rules and appear in Figure 5.b.

The velocity of the point A is given through the length of link 0 (the driver) and its angular velocity. The lines l_{F_x}, l_{F_y}, l_{A_x}, l_{A_y} are the lines passing through the points F and A and parallel to the x- and y-axis, respectively. For example,

$$l_{F_x} = F \vee i = \begin{Bmatrix} x_F \\ y_F \\ 1 \end{Bmatrix} \vee \begin{Bmatrix} 1 \\ 0 \\ 0 \end{Bmatrix} = \begin{Bmatrix} \begin{vmatrix} y_F & 0 \\ 1 & 0 \end{vmatrix} \\ -\begin{vmatrix} x_F & 1 \\ 1 & 0 \end{vmatrix} \\ \begin{vmatrix} x_F & 1 \\ y_F & 0 \end{vmatrix} \end{Bmatrix} = \begin{Bmatrix} 0 \\ 1 \\ -y_F \end{Bmatrix} \tag{16}$$

The rigidity matrix is obtained from the six equations given in Figure 5.b, written in the matrix-vector form as appears in Figure 5.c.

Generically the rigidity matrix has full rank 5 so that the mechanism is instantaneously controlled by the rotation of the driver link. This result is obtained because the driver constraint is included in the body-bar graph. If the driver link is considered as bar constraint, i.e. passive, the rigidity matrix would have only 5 rows and yield the generic DOF 1.

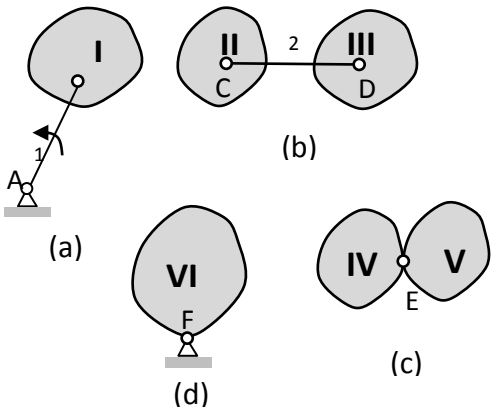

	I	...	II	...	III	...	IV	V	...	VI	...
1	$B \vee A$	...	0	...	0	...	0	0	...	0	...
⋮											
2	0	...	$C \vee D$	...	$D \vee C$	...	0	0	...	0	...
⋮											
$3 = E_x$	0	...	0	...	0	...	$E \vee i$	$i \vee E$	...	0	...
$4 = E_y$	0	...	0	...	0	...	$E \vee j$	$j \vee E$	...	0	...
⋮											
$5 = F_x$	0	...	0	...	0	...	0	0	...	$F \vee i$	...
$6 = F_y$	0	...	0	...	0	...	0	0	...	$F \vee j$	...
⋮											

(e)

Figure 4 Representing the different constraints in the body-bar rigidity matrix. a) The driver. b) Bar connecting two bodies. c) A revolute joint connecting two bodies. d) A pinned joint connecting the body to the ground. e) Body-bar rigidity matrix.

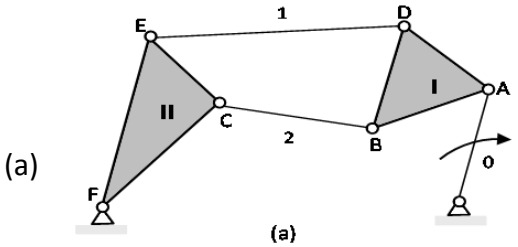

(b)

$$\begin{bmatrix} l_1 & -l_1 \\ l_2 & -l_2 \\ 0 & l_{F_x} \\ 0 & l_{F_y} \\ l_{A_x} & 0 \\ l_{A_y} & 0 \end{bmatrix} \begin{Bmatrix} Z_I \\ Z_{II} \end{Bmatrix} = \begin{Bmatrix} 0 \\ 0 \\ 0 \\ 0 \\ v_{A_x} \\ v_{A_y} \end{Bmatrix}$$

	v_{xI}	v_{yI}	ω_I	v_{xII}	v_{yII}	ω_{II}
1	$y_B - y_C$	$x_C - x_B$	$x_B y_C - x_C y_B$	$y_C - y_B$	$x_B - x_C$	$x_C y_B - x_B y_C$
2	$y_D - y_E$	$x_E - x_D$	$x_D y_E - x_E y_D$	$y_E - y_D$	$x_D - x_E$	$x_E y_D - x_D y_E$
F_x	0	0	0	0	1	$-y_F$
F_y	0	0	0	−1	0	x_F
A_x	0	1	$-y_A$	0	0	0
A_y	−1	0	x_A	0	0	0

(c)

Figure 5 The body-bar Stephenson type II, its governing equations and its body-bar rigidity matrix. a) Stephenson type II. b) The governing equations. c) The corresponding body-bar rigidity matrix.

4.4 The spatial body-bar rigidity matrix for mechanisms

In this section we introduce the rule for constructing the body-bar matrix in 3D. Due to space limitations we only present the constraints for a bar constraint.

Suppose we have two bodies, I and II and a constraint between them presented by a bar connected to the bodies at points A and B, respectively. This constraint will be written according to property 2.

Property 2: For the constraint between the two bodies there will be at most six entries written according to the following equation:

$$Z_I \vee (A \vee B) + Z_{II} \vee (B \vee A) = 0 \tag{17}$$

Proof of property 2: A hyperplane, denoted by *H*, in dimension d is a geometrical entity with dimension d-1 [32].Thus, in 2D it is a line while in 3D it is a plane. Its homogeneous coordinates are defined so, that the scalar product of the hyperplane with the point *P* is its distance from the hyperplane:

$$H = \begin{Bmatrix} \mathbf{n} \\ -d \end{Bmatrix} \qquad (18)$$
$$H \cdot P = \mathbf{n} \cdot \mathbf{P} - d$$

n is the normal to the hyperplane. If P is an origin, than *H·P=-d*, so *d* is simply the distance from the hyperplane to the origin.

One of the unique properties of a hyperplane is that when we apply to it the join operation of a point it is equal as performing a scalar product, as follows:

$$H \vee P = H \cdot P \qquad (19)$$

The join of two points is a weighted line, directed from the first point to the second, where the weight is the distance between the points and l is the unit vector from P to Q, as follows:

$$P \vee Q = |\mathbf{Q} - \mathbf{P}| l \qquad (20)$$

Now, we can define motion of a point through hyperplane, as follows:

$$M(P) = \begin{Bmatrix} \mathbf{v}_P \\ -\mathbf{P} \cdot \mathbf{v}_P \end{Bmatrix} = v_P \begin{Bmatrix} \mathbf{n}_P \\ -\mathbf{P} \cdot \mathbf{n}_P \end{Bmatrix} \qquad (21)$$

Where $\mathbf{v}_P$ is the velocity of the point P and $\mathbf{n}_P$ is its direction unit. As can be seen from equation 16, the motion is a weighted hyperplane with a normal identical to the direction of the velocity.

As known in the literature [32]the motion of a point on a body is defined as the join of the center of motion, Z, and the point P as follows:

$$Z \vee P = M(P) \qquad (22)$$

In 2D the center of motion is a weighted point, which is an instantaneous center of rotation, and in 3D the center of motion is the weighted instantaneous screw axis.

The join of the motion of point P and a point Q can be defined:

$$M(P) \vee Q = (Z \vee P) \vee Q = Z \vee (P \vee Q) = |\mathbf{Q} - \mathbf{P}| Z \vee l \qquad (23)$$

Where |**Q**-**P**| is the distance between the points **P** and **Q**. Since the M(P) is a weighted hyperplane thus, according to equation (14), the join operation with point Q can be performed by a scalar product as follows:

$$M(P) \vee Q = \mathbf{v}_P \cdot \mathbf{Q} - \mathbf{P} \cdot \mathbf{v}_P = \mathbf{v}_P \cdot (\mathbf{Q} - \mathbf{P}) \qquad (24)$$

Where the last expression is the projection of the velocity of point P on the line from P to Q with the weight equals to the distance from P to Q. Thus, after comparing the last two equations it can be derived that the join between the center of motion with some line results in the projection of the velocity of the points on this line, as follows:

$$Z \vee l = v_{P|l} \qquad (25)$$

This is constant along this line.Now, let *l* be the line that defines the bar connecting between the two bodies, i.e., $l = A \vee B$ we have:

$$\mathrm{v}_{\mathrm{P|l}} = \mathrm{Z}_{\mathrm{I}} \vee \mathrm{l} = \mathrm{Z}_{\mathrm{II}} \vee \mathrm{l} \qquad (26)$$

$$\mathrm{Z}_{\mathrm{I}} \vee (\mathrm{A} \vee \mathrm{B}) = \mathrm{Z}_{\mathrm{II}} \vee (\mathrm{A} \vee \mathrm{B}) \qquad (27)$$

$$\mathrm{Z}_{\mathrm{I}} \vee (\mathrm{A} \vee \mathrm{B}) + \mathrm{Z}_{\mathrm{II}} \vee (\mathrm{B} \vee \mathrm{A}) = 0 \qquad (28)$$

Equation (28) defines the construction rule for writing the body-bar rigidity matrix for any mechanism. Note, equation (10) is a special case of equation (28) as is derived as follows: a line is a hyperplane in 2D thus the joint between Z and the line in equation (26) can be written as an inner product, explained in equation (14), yielding equation (10).

For spatial mechanisms the center of motion is a line, termed ISA (instantaneous screw axis) defined as follows:

$$Z = \begin{Bmatrix} \omega \mathbf{t} \\ \omega \mathbf{m} + v \mathbf{t} \end{Bmatrix} \qquad (29)$$

Where **t** is the direction of the ISA, **m** is the moment of the ISA, ωis the instantaneous angular velocity around the ISA and *v* is the instantaneous translational velocity along the ISA [35]

Example: Body-Bar Rigidity Matrix of Stewart Platform

In the light of rigidity body-bar concept, Stewart platform consists of two bodies: the ground and the platform and six bars, this time can change their lengths, connecting between the two bodies. In this example the platform is designated by A and the ground by B and bar i is defined by two points where it is connected to the bodies, Ai and Bi. The governing equation for calculating the velocity of each bar is [32]:

$$Z \vee (A \vee B) = Z \cdot \begin{Bmatrix} \mathbf{B} \times \mathbf{A} \\ \mathbf{A} - \mathbf{B} \end{Bmatrix} \qquad (30)$$

From the latter equation it is possible to derive the projection of each point of body A, let it be Ai, on the line of the bar connected to it, l_i, as follows:

$$v_{A_i|l_i} = Z \vee (A_i \vee B_i) \frac{1}{|\mathbf{A}_i - \mathbf{B}_i|} = Z \cdot \begin{Bmatrix} \mathbf{B}_i \times \mathbf{A}_i \\ \mathbf{A}_i - \mathbf{B}_i \end{Bmatrix} \frac{1}{|\mathbf{A}_i - \mathbf{B}_i|} = v_i \qquad (31)$$

where v_i is the given velocity of bar i. Based on equation (31) it is possible to construct the body-bar rigidity matrix corresponding to the Stewart Platform appearing in figure 7.

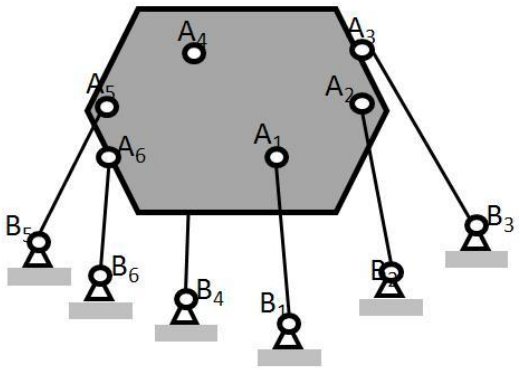

Figure 7 The schematic description of the Stewart Platform.

According to equation (31), the corresponding body-bar of the Steart Platform can be constructed as follows:

$$\begin{bmatrix}
\frac{(\mathbf{B}_1\times\mathbf{A}_1)_x}{L_1} & \frac{(\mathbf{B}_1\times\mathbf{A}_1)_y}{L_1} & \frac{(\mathbf{B}_1\times\mathbf{A}_1)_z}{L_1} & \frac{(\mathbf{A}_1-\mathbf{B}_1)_x}{L_1} & \frac{(\mathbf{A}_1-\mathbf{B}_1)_y}{L_1} & \frac{(\mathbf{A}_1-\mathbf{B}_1)_z}{L_1} \\
\frac{(\mathbf{B}_2\times\mathbf{A}_2)_x}{L_2} & \frac{(\mathbf{B}_2\times\mathbf{A}_2)_y}{L_2} & \frac{(\mathbf{B}_2\times\mathbf{A}_2)_z}{L_2} & \frac{(\mathbf{A}_2-\mathbf{B}_2)_x}{L_2} & \frac{(\mathbf{A}_2-\mathbf{B}_2)_y}{L_2} & \frac{(\mathbf{A}_2-\mathbf{B}_2)_z}{L_2} \\
\frac{(\mathbf{B}_3\times\mathbf{A}_3)_x}{L_3} & \frac{(\mathbf{B}_3\times\mathbf{A}_3)_y}{L_3} & \frac{(\mathbf{B}_3\times\mathbf{A}_3)_z}{L_3} & \frac{(\mathbf{A}_3-\mathbf{B}_3)_x}{L_3} & \frac{(\mathbf{A}_3-\mathbf{B}_3)_y}{L_3} & \frac{(\mathbf{A}_3-\mathbf{B}_3)_z}{L_3} \\
\frac{(\mathbf{B}_4\times\mathbf{A}_4)_x}{L_4} & \frac{(\mathbf{B}_4\times\mathbf{A}_4)_y}{L_4} & \frac{(\mathbf{B}_4\times\mathbf{A}_4)_z}{L_4} & \frac{(\mathbf{A}_4-\mathbf{B}_4)_x}{L_4} & \frac{(\mathbf{A}_4-\mathbf{B}_4)_y}{L_4} & \frac{(\mathbf{A}_4-\mathbf{B}_4)_z}{L_4} \\
\frac{(\mathbf{B}_5\times\mathbf{A}_5)_x}{L_5} & \frac{(\mathbf{B}_5\times\mathbf{A}_5)_y}{L_5} & \frac{(\mathbf{B}_5\times\mathbf{A}_5)_z}{L_5} & \frac{(\mathbf{A}_5-\mathbf{B}_5)_x}{L_5} & \frac{(\mathbf{A}_5-\mathbf{B}_5)_y}{L_5} & \frac{(\mathbf{A}_5-\mathbf{B}_5)_z}{L_5} \\
\frac{(\mathbf{B}_6\times\mathbf{A}_6)_x}{L_6} & \frac{(\mathbf{B}_6\times\mathbf{A}_6)_y}{L_6} & \frac{(\mathbf{B}_6\times\mathbf{A}_6)_z}{L_6} & \frac{(\mathbf{A}_6-\mathbf{B}_6)_x}{L_6} & \frac{(\mathbf{A}_6-\mathbf{B}_6)_y}{L_6} & \frac{(\mathbf{A}_6-\mathbf{B}_6)_z}{L_6}
\end{bmatrix}
\begin{Bmatrix}
\omega t_x \\ \omega t_y \\ \omega t_z \\ \omega m_x + v t_x \\ \omega m_y + v t_y \\ \omega m_z + v t_z
\end{Bmatrix} =
\begin{Bmatrix}
v_1 \\ v_2 \\ v_3 \\ v_4 \\ v_5 \\ v_6
\end{Bmatrix}$$

In the following section we introduce a special case of body-bar approach termed *bar-joint approach.*

5The Bar-Joint Approach to Mechanism Analysis

A bar-joint representation of a mechanism consists of binary links (the edges) that are connected by spherical joints (the vertices) in 3D and revolute joints in 2D, respectively. In so far a bar-joint graph resembles the physical system, but it must be noticed the vertices embody as many joints as necessary to link the attached bodies. A vertex connecting *k* edges (bodies) represents *k*-1 joints.

In this paper we show that this representation of mechanisms can formally be derived from the body-bar mechanisms by shrinking the bodies into joints. These mechanisms can be also viewed as mechanisms consisting of point masses that have only a pure translational motion. Although there exist methods and algorithms for checking the topological/generic mobility of body-bar mechanisms in 2D and 3D, for 3D bar-joint mechanisms there are no such algorithms. Furthermore, there are some 3D bar-joint mechanisms for which all the known algorithms provide with a wrong answer of their topologic/generic mobility. This strange phenomenon is explained more in details in the conclusion.

5.1 Deriving the bar-joint rigidity matrix from the body-bar rigidity matrix

Let us start from the equations developed for body-bar mechanisms (section 2.1.3), only this time the bodies are shrunk to joints, i.e., very small bodies with pure translation motion. In this case the center of motions of these small bodies is at infinity and the angular velocity is equal to zero, i.e., the three DOF of bodies are reduced to the two DOF of the joints.

Let us start from equation (4) but this time the third component of the center of motion is zero since it is at infinity, as shown in (12).

$$M_B(P) = \begin{Bmatrix} v_x \\ v_y \\ -v_x x_P - v_y y_P \end{Bmatrix} = Z \vee P = \begin{Bmatrix} Z_x \\ Z_y \\ 0 \end{Bmatrix} \vee \begin{Bmatrix} x_P \\ y_P \\ 1 \end{Bmatrix} = \begin{Bmatrix} Z_y \\ -Z_x \\ -Z_y x_P + Z_x y_P \end{Bmatrix} \qquad (32)$$

From equation (32) it follows that the center of motion of the joints is :

$$Z = \begin{Bmatrix} -v_y \\ v_x \\ 0 \end{Bmatrix} \qquad (33)$$

Let us apply equation (10) to a binary link whose end joints are A and B whose center of motion is defined by equation (33), resulting with the following equation:

$$0 = (Z_A - Z_B)\cdot(A \vee B) = \left(-v_{A_y} + v_{B_y}\right)(y_B - y_A) + \left(v_{A_x} - v_{B_x}\right)(x_A - x_B) = (\mathbf{v}_A - \mathbf{v}_B)\cdot(\mathbf{r}_A - \mathbf{r}_B) \qquad (34)$$

5.2 Rule for constructing the bar-joint rigidity matrix for mechanisms

Equation (34) defines the method to construct the rigidity matrix of any bar-joint mechanism. Each row corresponds to a binary link and two columns to a joint, each for the velocity in the x and y coordinate.

For the sake of clarity, we apply the rule appearing in equation (34) and construct the bar-joint rigidity matrix of the mechanism Stephenson type II, as appears in Figure 8.

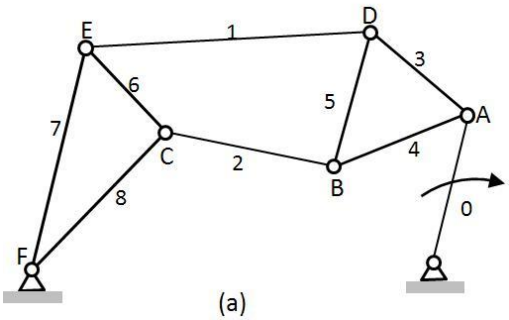

(a)

$$\begin{bmatrix} 0 & 0 & 0 & 0 & x_D-x_E & y_D-y_E & x_E-x_D & y_E-y_D \\ x_B-x_C & y_B-y_C & x_C-x_B & y_C-y_B & 0 & 0 & 0 & 0 \\ 0 & 0 & 0 & 0 & x_D-x_A & y_D-y_A & 0 & 0 \\ x_B-x_A & y_B-y_A & 0 & 0 & 0 & 0 & 0 & 0 \\ x_B-x_D & y_B-y_D & 0 & 0 & x_D-x_B & y_D-y_B & 0 & 0 \\ 0 & 0 & x_C-x_E & y_C-y_E & 0 & 0 & x_E-x_C & y_E-y_C \\ 0 & 0 & 0 & 0 & 0 & 0 & x_E-x_F & y_E-y_F \\ 0 & 0 & x_C-x_F & y_C-y_F & 0 & 0 & 0 & 0 \end{bmatrix}$$

(b)

Figure 8 The bar-joint Stephenson II (a) and its corresponding bar-joint rigidity matrix.

6. Computing the Generic Mobility with a combinatorial Algorithm – The Pebble Game

The problem of determining the correct generic mobility is well known in the literature, both in structures and in mechanisms. For example, in Figure there are two pinned bar – joints graphs, both having the same number of vertices and edges. However, among them there is a disparity which is as follows: the graph in Figure 9a has one DOF and has a finite motion, while the one in Figure 9b is a rigid graph, immobile.

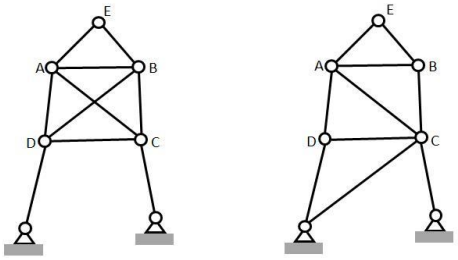

(a) (b)

Figure 9 Example of two pinned graphs for which CKG equation results in the same DOF. (a) Mechanism with redundant region; (b) Rigid truss.

The problem of determining the generic mobility for 2D bar-joint was solved only in 1997, by two physicists: Jacobs and Hendrickson. Their main aim was to develop an algorithm for checking whether a graph is rigid, i.e., whether it has zero generic mobility. As we show here, this algorithm was found to be applicable other important problems related to generic mobility. This algorithm is called the pebble game [10] and is described in the following sections.

Remark: Although body-bar and bar-joint graphs are equivalent representations of the mechanism topology there is an important difference for the application of the pebble game. It is was proved [13] that the pebble game always finds the correct generic mobility for body-bar graphs, but it may fail for bar-joint graphs. For simplicity, in this section the pebble game is described for the bar-joint graph. The algorithm proceeds similarly for the body-bar graph.

6.1 The combinatorial algorithms for computing the generic mobility – Pebble game

Let G=(V,E) be a bar and joint graph. Each vertex is given two pebbles, corresponding to the two degrees of freedom that a point in a planar system has. A vertex can use its pebbles to cover any two edges which are incident to that vertex.

When an edge is directed, one constraint is added; therefore one degree of freedom is removed from the total system (one pebble). Every ungrounded system, i.e. a floating system, must contain at least 3 DOFs (of a body in plane), therefore three pebbles are always present in the graph. To direct an edge four edges should be on its end vertices, two on each vertex as shown in figure 10. The edge is being directed by moving one pebble to the edge, defining a constraint between its two end vertices.

(a) (b)

Figure 10 Example of assigning a pebble to an edge (constraint) (a) Two pebbles should be at the end vertices. (b) The constraint was added and the edge is directed.

Once four pebbles are located at the end vertices of the desired edge, we are guaranteed that these points are independent in the plane, and that adding an edge between them will not result in an over constrained system. The fact that four pebbles are necessary is used in the algorithm by quadrupling the edge under test before it is being directed. In case the independence test is successful, the edge can then be directed, i.e., a constraint is added between these points, and one degree of freedom is reduced from the total system (one pebble is used to mark the edge). In fact, this operation defines a constant distance between the end vertices, and this constraint equals to one DOF.

The mains steps of the algorithms:

1. **Arbitrarily pick a starting vertex**.

2. **There are two types of moves possible:**

2.1 **Direct an edge move**: If i and j are vertices with two pebbles on each, i.e., the vertices are independent and there is no constraint between them, then assign one pebble from one of the end vertices to the edge, suppose from vertex i (wlog). The edge (i,j) is now directed from i to j, i.e., <i,j>.

In case two pebbles cannot be found at the ends of that constraint, after an exhaustive search, this edge is marked as a redundant.

2.2 **Pebble slide move**: If there is a constraint between vertex i and vertex j, then there exists a directed edge <i,j>and there must be a pebble on j. What we do is reverse the direction of the edge so that it is now directed from j to i and move the pebble from j to i.

The algorithm ends when all the edges have been processed (directed or not).

For the sake of clarity, let us see how the Pebble game concludes that the floating Bar-Joint graph – the triangle

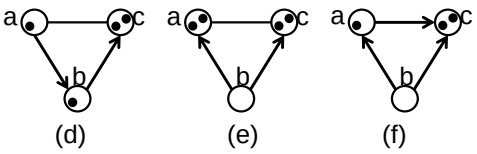

(figure 11

Figure 11a) is rigid. First, two pebbles are assigned to each vertex, Figure 11b. Edge (a,b) can be directed since there are two pebbles in each of its end vertices as shown in Figure 11.c, the same is true for edge (b,c), Figure 11.d. In order to direct the edge (a,c), two pebbles should be moved to its end vertices. Therefore a pebble from vertex b moves to vertex a and the direction of (a,b) is swapped, Figure 11.e. Now (a,c) is directed, Figure 11.f. Now that all edges have been processed, all edges are directed and there are 3 free pebbles on the graph (3 DOF of a rigid body), and in fact, the graph is indeed rigid, without over-constraints.

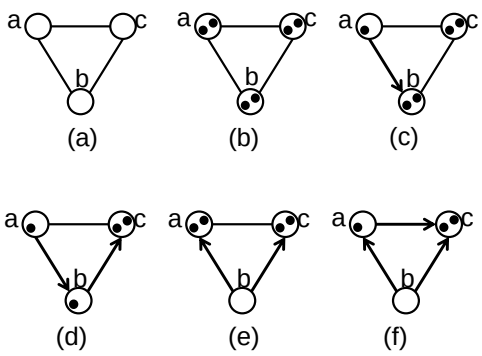

Figure 11 Example of applying the Pebble game for validating the rigidity of a triangle. (a) undirected graph G (b) each vertex is given 2 pebbles (c) ,(d), (f) direct an edge move (e) pebble slide move. Minimally rigid graph, three free pebbles left.

6.2 Determining all the redundant links via the pebble game

One of the benefits of the pebble game algorithm is that it allows to determine the regions where there is a topological redundancy. In this case, redundant edges will fail to be directed since an exhaustive search will not succeed to move two pebbles to each end vertex of the edge.

We will explain how the Pebble game finds the redundant region through an example appearing in figure 12. At first all the vertices are given two pebbles, figure 12a. After several pebble moves, all edges except (B,D) have been directed and only three pebbles are left so there is no possibility to assign a pebble to edge (B,D) as explained above.

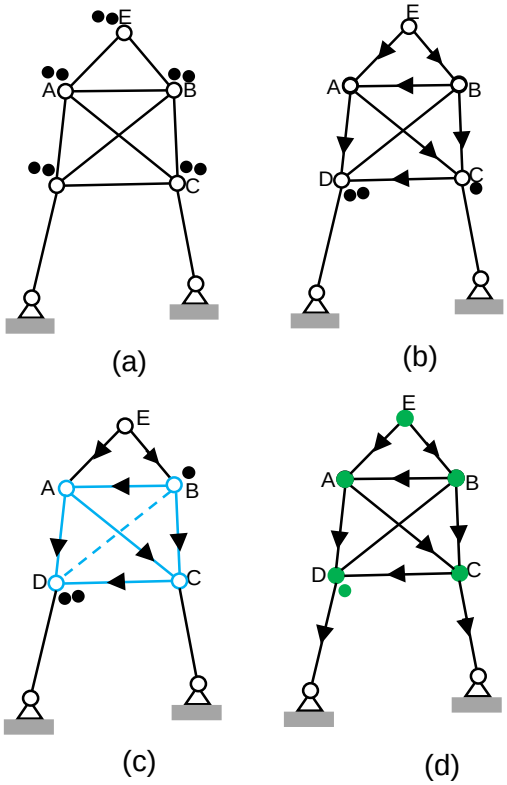

Figure 1 Example of revealing a topological redundancy region and generic mobility of joints by the pebble game.(a) Initial state for pebble game. (b) Directing all the possible edges. (c) The redundant region, colored in blue. d) The joints with one topological DOF are colored in green.

6.3 Determining the topological DOF of joints by the Pebble game

After pebble game assigns maximum inner edges the free pebbles that are left are moved to the ground, each ground edge is assigned same as before with one pebble and is

directed towards the ground. The free pebbles left in the graph after directing the ground edges define the topological DOF of each joint, as follows: for each joint move the maximum number of free pebbles as possible. The maximum number of free pebbles that can be moved to a joint determines its topological DOF. As an example, in Figure 12.d it is possible to move to each joint a maximum of one pebble, in the figure located next to joint D, thus all the joints in this example have one topological DOF.

A case where there are no pebbles left can be seen in figure 13.b, thus all the joints are topologically immobile, i.e., the structure is rigid.

The redundant region is found as follows: Let v be the vertex whose maximum pebbles that can be moved to is less than two pebbles. As an example, vertex B in figure 12.c is such a vertex. All the vertices to which there is a directed path, a sequence of directed edges, from vertex B are marked, in figure 12 they are colored with blue. All the edges whose end vertices are colored with blue are the redundant edges, i.e., removing each one of them does not affect the generic mobility of the graph.A graph with no redundant edges is given in figure 13a, and the Pebble algorithm results with this conclusion since all the edges are directed as shown in Figure 13b

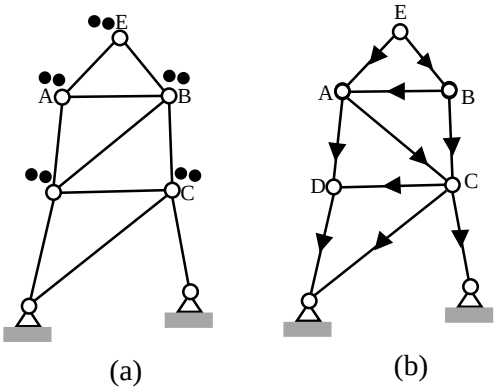

Figure 2 Example of proving the rigidity of a structure.
(a) Initial state for pebble game. (b) All the edges are directed.

7. Summary

In this paper the body-bar and bar-joint representation of mechanism kinematics has been revisited. Each one of these representations gives rise to one type of rigidity matrix. The geometric rules for constructing these matrices are derived. They have been known for mechanism only comprising revolute respectively spherical joints. Here a novel formulation of body-bar rigidity matrix that also applies in-line and prismatic joints of planar mechanisms is reported. This allows, for the first time treating general planar mechanisms with the body-bar approach.Further the rigidity matrix of spatial mechanisms is derived when, at the moment, only spherical joints are assumed. It is shown how the rigidity matrices allow for mobility calculation. This yields the generic mobility, and when evaluated for a specific geometry the rigidity matrix yields the instantaneous mobility of a particular mechanism.

A further significance of the two types of representation is that they enable computation of the generic mobility via a combinatorial method called the pebble game. This algorithm is explained in the paper. The fact that the pebble game always finds the correct generic mobility if applied to body-bar graphs has far reaching consequences for the mobility determination since it overcomes the limitation of the Chebyshev-Kutzbach-Grübler formula.

It was further shown in this paper that the bar-joint is a special case of body-bar representation.

Appendix

A. Topics of projective geometry underlying this method

The motion of a rigid body in the plane can be expressed as a rotation, with angular velocity ω, about its instantaneous center of motion. Denote with $C=(x_c\ y_c\ 1)$ the homogenous coordinates of the instantaneous center of motion with Cartesian coordinates x_c, y_c.For later use introduce the abbreviation

$$Z=\begin{Bmatrix}\omega x_c\\ \omega y_c\\ \omega\end{Bmatrix}=\omega\begin{Bmatrix}x_c\\ y_c\\ 1\end{Bmatrix}=\omega C \tag{35}$$

The join operation on two points P and Q defines a line *l* from P to Q. Its projective coordinates are calculated as the minors as follows:

$$l=P\vee Q=\begin{Bmatrix}x_P\\ y_P\\ 1\end{Bmatrix}\vee\begin{Bmatrix}x_Q\\ y_Q\\ 1\end{Bmatrix}=\begin{Bmatrix}\begin{vmatrix}y_P & y_Q\\ 1 & 1\end{vmatrix}\\ -\begin{vmatrix}x_P & x_Q\\ 1 & 1\end{vmatrix}\\ \begin{vmatrix}x_P & x_Q\\ y_P & y_Q\end{vmatrix}\end{Bmatrix}=\begin{Bmatrix}y_P-y_Q\\ x_Q-x_P\\ x_Py_Q-x_Qy_P\end{Bmatrix} \tag{36}$$

The homogeneous form of the projective coordinates of the line is:

$$l=\begin{Bmatrix}-\sin\alpha\\ \cos\alpha\\ -d\end{Bmatrix} \tag{37}$$

Where α is the angle between the line and the *x*-axis and *d* is the distance from the origin to the line. The first two coordinates of the triple define the unit vector normal to the line.

The velocity of a point P in homogenous coordinates can be expressed as

$$Z \vee P = \begin{Bmatrix} \omega(y_C - y_P) \\ \omega(x_P - x_C) \\ \omega(x_C y_P - x_P y_C) \end{Bmatrix} = \begin{Bmatrix} v_{P_x} \\ v_{P_y} \\ -\mathbf{v}_P \cdot \mathbf{r}_P \end{Bmatrix} = |\mathbf{v}_P| \begin{Bmatrix} \hat{\mathbf{n}}_P \\ -d \end{Bmatrix} \quad (38)$$

where $\mathbf{v}_P$ is the velocity of the point P,$\mathbf{r}_P$the coordinate vector of point and $\hat{\mathbf{n}}_p$ is the normal unit vector in the direction of the velocity $\mathbf{v}_P$. Since the scalar product of the normal unit vector by the coordinate vector of point P is equal to the distance of the line through C and P from the origin, i.e., $d = \mathbf{n}_P \cdot \mathbf{r}_P$, the distance d appears in equation 4.

The triplet in equation (38) is termed in the literature as the *motion of point P*, and is denoted by $M_B(P)$ [32].

References

[1] K. Arikawa: Mobility Analysis of Robotic Mechanisms based on Computer Algebra, IDETC/CIE 2009, August 30 - September 2, 2009, San Diego, California, USA, DETC2009-87288

[2] J.E. Baker: Overconstrained six-bars with parallel adjacent joint-axes, Mech. Mach. Theory, vol. 38, 2003, pp. 103-107

[3] G.T. Bennett: The Skew Isogram Mechanism, Proc. London Math. Soc., vol. 13, no. 2, pp 151-173

[4] G. Gogu, Mobility of mechanism: a critical review, Mech. Mach. Theory vol. 40 ,2005, pp. 1068–1097

[5] G.Gogu: Structural Synthesis of Parallel Robots, Part 1: Methodology, Springer, 2008

[6] G.Gogu: Structural Synthesis of Parallel Robots, Part 2: TranslationalTopologies with Two and Three Degrees of Freedom, Springer, 2009

[7] J.M. Hervé: AnalyseStructurelle des Mécanismes par Groupe des Déplacements, Mech. Mach. Theory, vol. 13, 1978, pp. 437-450

[8] J.M. Hervé: Intrinsic formulation of problems of geometry and kinematics of mechanisms, Mech. Mach. Theory, vol. 17, No. 3, 1982, pp. 179-184

[9] M.L. Husty, H.-P. Schröcker: A Proposal for a new Definition of the Degree of Freedom of a Mechanism, IAK 2008, Conference on Interdisciplinary Applications of Kinematics, January 9-11, 2008, Lima, Peru

[10] D.J. Jacobs,B. Hendrickson: An Algorithm for Two-Dimensional Rigidity Percolation: The Pebble Game,Journal of Computational Physics, vol 137, No. 2, Nov. 1,1997.

[11] K. Kutzbach: Mechanische Leitungsverzweigung, ihre Gesetze und Anwendungen, Maschinenbau. Der Betrieb. vol. 8, 1929, pp. 710-716

[12] G. Laman: On graphs and the rigidity of plane skeletal structures, J. Engineering Mathematics, vol.4, No. 4, 1970, pp. 331–340

[13] A. Lee, I. Streinu:Pebble Game Algorithms and (k, l)-Sparse Graphs, proc. EuroComb 2005, DMTCS proc. A.E. 2005, pp. 181-186.

[14] L. Lovász and Y. Yemini:.On Generic rigidity in the plane, SIAM J. Alg. Disc.Methodsvol. 3, no.1, 1982, pp. 91–98.

[15] C. Mavroidis, B. Roth: Analysis of Overconstrained Mechanisms, ASME J. Mech. Design, vol. 117, 1995, pp. 69-74

[16] C. Mavroidis, B. Roth: New and Revised Overconstrained Mechanisms, ASME J. Mech. Design, vol. 117, 1995, pp. 75-82

[17] A. Müller: Generic Mobility of Rigid Body Mechanisms, Mechanism and Machine Theory, Vol. 44, no. 6, June 2009, pp. 1240-1255

[18] A. Müller: On the Concept of Mobility used in Robotics, 33rd Mechanisms & Robotics Conference, ASME 2009 International Design Engineering Technical Conferences, August 30 – September 2, 2009, San Diego, CA, USA

[19] A. Müller, J.M. Rico: Mobility and Higher Order Local Analysis of the Configuration Space of Single-Loop Mechanisms, in: J. J. Lenarcic, P. Wenger (eds.), Advances in Robot Kinematics, 2008, Springer, pp. 215-224

[20] A. Müller, S. Piipponen: The Geometric vs Algebraic Definition of Mobility, 13th World Congress in Mechanism and Machine Science, Guanajuato, Mexico, 19-25 June, 2011

[21] J.M. Rico Martinez, B. Ravani: On mobility analysis of linkages using group theory, ASME J. Mech. Des. vol. 135, 2003, pp. 70-80

[22] B. Servatius, O.Shai,W.Whiteley: Geometric Properties of Assur Graphs, European Journal of Combinatorics, vol. 31, No. 4, May,2010, pp. 1105-1120.

[23] A. Sljoka, O Shai, W. Whiteley:Checking mobility and decomposition of linkages via Pebble Game Algorithm, ASME Design Engineering Technical Conferences, August 28-31,2011,Washington,USA.

[24] H. Stachel: A proposal for a proper definition of higher-order rigidity, Tensegrity Workshop 2007, July 9 13, 2007, La Vacquerie,France.

[25] T.-S. Tay: Rigidity of multigraphs I: linking rigid bodies in n-space. Journal of Combinatorial Theory Series, B vol26,1984,pp.95–112

[26]M.F.Thorpe,P.M.Duxbury, edi.: Rigidity Theory and Applications, Kluwer Academic /Plenum publishers, NY, 1999.

[27] K.J. Waldron: The constraint analysis of mechanisms, J. Mech. vol. 1, 1966, pp. 101-114

[28] K.J. Waldron: A Study of Overconstrained Linkage Geometry by Solution of Closure Equations - Part I. Method of Study, Mech. Mach. Theory, vol. 8, 1973, pp. 95-104

[29] K.J. Waldron: A Study of Overconstrained Linkage Geometry by Solution of Closure Equations - Part II. Four-Bar Linkages with Lower Pairs other than Screw Joints, Mech. Mach. Theory, vol. 8, 1973, pp. 233-247

[30] C. Wampler, B.T. Larson, A.G. Erdman: A new Mobility Formula for spatial Mechanisms, Proc. ASME International Design Engineering Technical Conferences (IDETC), Sep. 4-7, 2007, Las Vegas,USA.

[31]W. Whiteley: Rigidity and Scene Analysis. in Handbook of Discreteand Computational Geometry, 2nd Edition J. O'Rourke,J. Goodman (eds): 1327-1354, 2004.

[32] N. White,W.Whiteley: The algebraic geometry of motions of bar-and-body frameworks. SIAM J. Algebraic Discrete Methods, 8(1):1-32,1987.

[33] K. Wohlhart: Kinematotropic Linkages, in: J. Lenarcic, V. Parent-Castelli (eds.): Recent Advances in Robot Kinematics, Kluwer, 1996, pp. 359-368

[34] Jing-Shan Zhao et al: Computation of the configuration degree of freedom of a spatial parallel mechanism by using reciprocal screw theory, Mech. Mach. Theory, vol. 41, 2006, pp. 1486-1504

[35] Bottema, O, B. Roth: Theoretical Kinematics, Dover, 1990